Effect of Mutations in the Cytochrome *b ef* Loop on the Electron-Transfer Reactions of the Rieske Iron−Sulfur Protein in the Cytochrome bc_1 Complex†

Sany Rajagukguk,‡,§ Shaoqing Yang,‡,|| Chang-An Yu,|| Linda Yu,|| Bill Durham,§ and Francis Millett*,§

Department of Chemistry and Biochemistry, University of Arkansas, Fayetteville, Arkansas 72701, and Department of Biochemistry and Molecular Biology, Oklahoma State University, Stillwater, Oklahoma 74078

Received October 7, 2006; Revised Manuscript Received December 5, 2006

ABSTRACT: Long-range movement of the Rieske iron−sulfur protein (ISP) between the cytochrome (cyt) *b* and cyt c_1 redox centers plays a key role in electron transfer within the cyt bc_1 complex. A series of 21 mutants in the cyt *b ef* loop of *Rhodobacter sphaeroides* cyt bc_1 were prepared to examine the role of this loop in controlling the capture and release of the ISP from cyt *b*. Electron transfer in the cyt bc_1 complex was studied using a ruthenium dimer to rapidly photo-oxidize cyt c_1 within 1 μs and initiate the reaction. The rate constant for electron transfer from the Rieske iron−sulfur center [2Fe2S] to cyt c_1 was $k_1 = 60\,000\ s^{-1}$. Famoxadone binding to the Q_o site decreases k_1 to $5400\ s^{-1}$, indicating that a conformational change on the surface of cyt *b* decreases the rate of release of the ISP from cyt *b*. The mutation I292A on the surface of the ISP-binding crater decreased k_1 to $4400\ s^{-1}$, while the addition of famoxadone further decreased it to $3000\ s^{-1}$. The mutation L286A at the tip of the *ef* loop decreased k_1 to $33\,000\ s^{-1}$, but famoxadone binding caused no further decrease, suggesting that this mutation blocked the conformational change induced by famoxadone. Studies of all of the mutants provide further evidence that the *ef* loop plays an important role in regulating the domain movement of the ISP to facilitate productive electron transfer and prevent short-circuit reactions.

The cytochrome (cyt)[1] bc_1 complex (ubiquinol:cyt *c* reductase) is an integral membrane protein in the electron-transport chains of mitochondria and many respiratory and photosynthetic prokaryotes (*1*, *2*). The complex contains the Rieske iron−sulfur protein (ISP), cyt c_1, and two *b*-type hemes (b_L and b_H) in the cyt *b* subunit (*1*, *2*). The complex translocates four protons to the positive side of the membrane as two electrons are transferred from ubiquinol (QH_2) to cyt *c* using a widely accepted Q-cycle mechanism (*2*). In a key bifurcated reaction, QH_2 binds to the Q_o site located near the outside of the membrane and transfers its first electron to the Rieske iron−sulfur center ([2Fe2S]) and then to cyt c_1 and cyt *c* (*1*, *2*). The second electron is transferred from semiquinone in the Q_o site to cyt b_L and then to cyt b_H, leading to the reduction of ubiquinone in the Q_i site to the semiquinone. This cycle is repeated to reduce the semiquinone at the Q_i site to QH_2. A recent freeze-quench electron paramagnetic resonance (EPR) study has shown that QH_2 reduced [2Fe2S] and cyt b_L simultaneously with a half-time of 250 μs, providing direct evidence for the bifurcation mechanism and indicating that either the semiquinone is very short-lived or the reaction is concerted (*3*). X-ray crystallographic studies have shown that the conformation of the ISP depends upon the presence of inhibitors in the Q_o site as well as the crystal form (*4*−*7*). An anomalous signal for [2Fe2S] is found close to cyt b_L in native $I4_122$ bovine crystals, but its intensity is small, indicating that the ISP is conformationally mobile (*4*, *7*). In beef, chicken, and yeast cyt bc_1 crystals grown in the presence of stigmatellin, the ISP is in a conformation with [2Fe2S] proximal to the cyt b_L heme, called the *b* state (*5*−*8*). However, in native chicken or beef $P6_522$ crystals in the absence of Q_o-site inhibitors, the ISP is in a conformation with [2Fe2S] close to cyt c_1, called the c_1 state (*5*, *6*). A novel shuttle mechanism for the ISP has been proposed on the basis of these structural studies (*4*−*7*). With the ISP initially in the *b* state, QH_2 in the Q_o site transfers an electron to the oxidized [2Fe2S] center. The ISP then rotates by 57° to the c_1 state, where reduced [2Fe2S] transfers an electron to cyt c_1. The main features of this mobile shuttle mechanism have been supported by a variety of experimental studies using mutation and/or cross-linking to immobilize the ISP or alter the conformation of the neck region (*9*−*20*).

An important question regarding the Q-cycle mechanism is how QH_2 at the Q_o site can deliver two electrons sequentially to the high- and low-potential chains, even though thermodynamics would favor the delivery of both electrons to the high-potential chain (*1*, *2*). A number of mechanisms have been proposed in which the conformations of the ISP and/or the quinone substrates are controlled to favor the reversible oxidation of QH_2 and minimize short-circuit reactions (*21*−*29*). Studies of the effects of Q_o-site inhibitors have indicated that there is a linkage between the

† This work was supported by NIH Grants GM20488 (to F.M. and B.D.), NCRR COBRE 1 P20 RR15569 (to F.M. and B.D.), and GM30721 (to C.-A.Y.).

* To whom correspondence should be addressed. Telephone: 479-575-4999. Fax: 479-575-4049. E-mail: millett@comp.uark.edu.

‡ These authors contributed equally to this study.

§ University of Arkansas.

|| Oklahoma State University.

[1] Abbreviations: cyt, cytochrome; ISP, Rieske iron−sulfur protein; [2Fe2S], Rieske iron−sulfur center; Ru_2D, $[Ru(bpy)_2]_2(qpy)(PF_6)_4$; qpy, 2,2′:4′,4″:2″,2‴-quaterpyridine; $Q_0C_{10}BrH_2$, 2,3-dimethoxy-5-methyl-6-(10-bromodecyl)-1,4-benzoquinol; SCR, succinate cytochrome *c* reductase.

10.1021/bi062094g CCC: $37.00
Published on Web 01/25/2007

Table 1: Primers Used during Mutagenesis Operations

mutant (in the cyt *b*)	primers
H276A (D252)	5′-GCCGAACTACCTCGGCGCCCCCGACAACTACATCG-3′
	3′-CGGCTTGATGGAGCCGCGGGGGCTGTTGATGTAGC-5′
P277A (P253)	5′-CGAACTACCTCGGCCACGCCGACAACTACATCGAGG-3′
	3′-GCTTGATGGAGCCGGTGCGGCTGTTGATGTAGCTCC-5′
D278A (D254)	5′-CTACCTCGGCCACCCCGCCAACTACATCGAGGCGAAC-3′
	3′-GATGGAGCCGGTGGGGCGGTTGATGTAGCTCCGCTTG-5′
D278N	5′-CTACCTCGGCCACCCCAACAACTACATCGAGGCGAAC-3′
	3′-GATGGAGCCGGTGGGGTTGTTGATGTAGCTCCGCTTG-5′
D278E	5′-CTACCTCGGCCACCCCGAAAACTACATCGAGGCGAAC-3′
	3′-GATGGAGCCGGTGGGGCTTTTGATGTAGCTCCGCTTG-5′
D278I	5′-CTACCTCGGCCACCCCATCAACTACATCGAGGCGAAC-3′
	3′-GATGGAGCCGGTGGGGTAGTTGATGTAGCTCCGCTTG-5′
D278H	5′-CTACCTCGGCCACCCCCACAACTACATCGAGGCGAAC-3′
	3′-GATGGAGCCGGTGGGGGTGTTGATGTAGCTCCGCTTG-5′
N279A (N255)	5′-CTCGGCCACCCCGACGCCTACATCGAGGCGAACCC-3′
	3′-GAGCCGGTGGGGCTGCGGATGTAGCTCCGCTTGGG-5′
Y280A (Y256)	5′-GGCCACCCCGACAACGCCATCGAGGCGAACCCGC-3′
	3′-CCGGTGGGGCTGTTGCGGTAGCTCCGCTTGGGCG-5′
L286A (L262)	5′-CATCGAGGCGAACCCGGCCTCGACGCCCGCGCAC-3′
	3′-GTAGCTCCGCTTGGGCCGGAGCTGCGGGCGCGTG-5′
L286E	5′-CATCGAGGCGAACCCGGAGTCGACGCCCGCGCAC-3′
	3′-GTAGCTCCGCTTGGGCCTCAGCTGCGGGCGCGTG-5′
L286I	5′-CATCGAGGCGAACCCGATCTCGACGCCCGCGCAC-3′
	3′-GTAGCTCCGCTTGGGCTAGAGCTGCGGGCGCGTG-5′
S287A (N263)	5′-CGAGGCGAACCCGCTCGCCACGCCCGCGCACATCG-3′
	3′-GCTCCGCTTGGGCGAGCGGTGCGGGCGCGTGTAGC-5′
A290S (A266)	5′-CCGCTCTCGACGCCCTCGCACATCGTGCCGG-3′
	3′-GGCGAGAGCTGCGGGAGCGTGTAGCACGGCC-5′
H291A (H267)	5′-GCTCTCGACGCCCGCGGCCATCGTGCCGGAATGG-3′
	3′-CGAGAGCTGCGGGCGCCGGTAGCACGGCCTTACC-5′
I292A (I268)	5′-CTCGACGCCCGCGCACGCCGTGCCGGAATGGTACTTC-3′
	3′-GAGCTGCGGGCGCGTGCGGCACGGCCTTACCATGAAG-5′
I292L	5′-CTCGACGCCCGCGCACCTGGTGCCGGAATGGTACTTC-3′
	3′-GAGCTGCGGGCGCGTGGACCACGGCCTTACCATGAAG-5′
I292M	5′-CTCGACGCCCGCGCACATGGTGCCGGAATGGTACTTC-3′
	3′-GAGCTGCGGGCGCGTGTACCACGGCCTTACCATGAAG-5′
I292V	5′-CTCGACGCCCGCGCACGTCGTGCCGGAATGGTACTTC-3′
	3′-GAGCTGCGGGCGCGTGCAGCACGGCCTTACCATGAAG-5′
I292E	5′-CTCGACGCCCGCGCACGAGGTGCCGGAATGGTACTTC-3′
	3′-GAGCTGCGGGCGCGTGCTCCACGGCCTTACCATGAAG-5′
I292R	5′-CTCGACGCCCGCGCACCGCGTGCCGGAATGGTACTTC-3′
	3′-GAGCTGCGGGCGCGTGGCGCACGGCCTTACCATGAAG-5′

occupant of the Q_o site and the conformation and dynamics of the ISP. Stigmatellin forms a hydrogen bond with the His-161 ligand of the [2Fe2S] center, thus increasing its redox potential by 200−250 mV and immobilizing the ISP in the *b* conformation (*5*−*8*, *30*). Famoxadone binding to the Q_o site leads to significant conformational changes on the surface of cyt *b*, which trigger a long-range conformational change in the ISP from the mobile state to a state with [2Fe2S] proximal to cyt *b* (*31*). The *ef* loop plays an important role in relaying conformational changes in the Q_o pocket to surface domains that control the binding of the ISP. Moreover, molecular dynamics simulations have shown that residues 263−268 of the *ef* loop are displaced by up to 2 Å as the ISP rotates from the *b* state to the c_1 state (*32*). In this paper, the effects of mutations of *ef* loop residues on electron transfer from QH_2 to the iron−sulfur center and then to cyt c_1 are studied using the binuclear ruthenium complex, $[Ru(bpy)_2]_2(qpy)(PF_6)_4$ (Ru_2D), where qpy is 2,2′:4′,4″:2″,2‴-quaterpyridine, to rapidly photo-oxidize cyt c_1 and initiate the reaction (*9*, *17*). The ruthenium photo-oxidation method provides a unique way to measure the dynamics of the ISP domain movement from the *b* state to the c_1 state (*9*, *17*, *33*).

EXPERIMENTAL PROCEDURES

Materials. A modification of the method of Downard et al. (*34*) was used to prepare Ru_2D. Succinate, *p*-benzoquinone, and antimycin A were obtained from Sigma Chemical Co.; stigmatellin was purchased from Fluka Chemical Co.; and *N*-dodecyl-*β*-D-maltoside was obtained from Anatrace. $[Co(NH_3)_5Cl]^{2+}$ was synthesized as described in ref *35*, and 2,3-dimethoxy-5-methyl-6-(10-bromodecyl)-1,4-benzoquinol ($Q_0C_{10}BrH_2$) was prepared as previously reported (*36*). Succinate cyt *c* reductase (SCR) was purified as previously described (*37*).

Generation of Rhodobacter sphaeroides Strains Expressing the His6-Tagged bc_1 Complexes. The Quickchange XL site-directed mutagenesis kit from Stratagene was employed for mutagenesis. Plasmid pGEM7Zf(+)-fbcB was used as a template, and forward and reverse primers were used for polymerase chain reaction (PCR) amplification. Template plasmid pGEM7Zf(+)-fbcB was constructed by ligating the fragment between *Nsi*I and *Xba*I in the plasmid pRKD-fbcFBC_{6H}Q into *Nsi*I and *Xba*I sites of the pGEM7ZF(+) plasmid. The primers used are listed in Table 1.

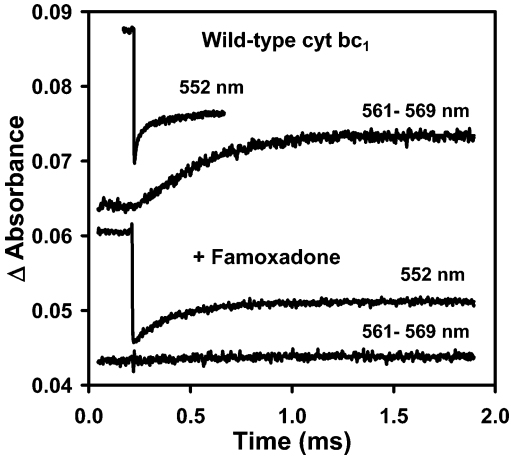

FIGURE 1: Electron transfer within wild-type *R. sphaeroides* cyt bc_1 following photo-oxidation of cyt c_1 (*9*). The 300 μL sample contained 5 μM cyt bc_1, 20 μM Ru_2D, and 5 mM $[Co(NH_3)_5Cl]^{2+}$ in 20 mM sodium borate at pH 9.0 with 0.01% dodecylmaltoside. The cyt bc_1 was treated with 10 μM $Q_oC_{10}BrH_2$, 1 mM succinate, and 50 nM SCR to completely reduce [2Fe2S] and cyt c_1 and reduce cyt b_H by about 30%. The sample was then excited with a 480 nm laser flash to photo-oxidize cyt c_1 within 1 μs. (Top two traces) The 552 nm transient indicates that cyt c_1 was photo-oxidized within 1 μs and then reduced in a biphasic reaction with rate constants of 60 000 and 2000 s^{-1}. The rate constant for the reduction of cyt b_H measured at 561−569 nm was 2300 s^{-1}. (Bottom two traces) The addition of 30 μM famoxadone decreased the rate of reduction of cyt c_1 to 5400 s^{-1} and eliminated the reduction of cyt b_H.

Scheme 1

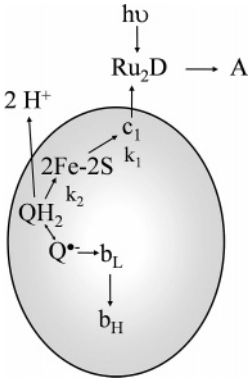

After mutagenesis, the *Nsi*I−*Xba*I fragment from the pGEM7Zf(+)-fbcBm was ligated into *Nsi*I and *Xba*I sites of the $pRKDfbcFB_{bpKm}C_{6H}$ plasmids, which contained the Kanamycin-resistant gene in the *Bst*I and pinA sites (*38*). Strains containing recombinant plasmid will be sensitive to antibiotic kanamycin. The $pRKDfbcFBmC_{6H}Q$ plasmid in *Escherichia coli* S17-1 cells was mobilized into *R. sphaeroides* BC-17 through conjugation (*38*). The engineered mutations were confirmed by DNA sequencing before and after photosynthetic growth as previously reported (*38*), which was performed by the Recombinant DNA/Protein Core Facility at Oklahoma State University, Stillwater, OK.

Mutant cyt bc_1 was purified as described by Xiao et al. (*39*). The steady-state activity of bc_1 complexes was determined as described by Liu et al. (*40*).

Flash Photolysis Experiments. Flash photolysis experiments were carried out on 300 μL solutions contained in a 1 cm glass semimicrocuvette using the detection system described by Heacock et al. (*41*). A Phase R model DL1400 flash lamp-pumped dye laser using coumarin LD 490 produced a 480 nm light flash of <0.5 μs in duration. Samples typically contained 5 μM cyt bc_1, 20 μM Ru_2D, and 5 mM $[Co(NH_3)_5Cl]^{2+}$ in 20 mM sodium borate at pH 9.0 and 0.01% dodecylmaltoside. $[Co(NH_3)_5Cl]^{2+}$ was used as a sacrificial electron acceptor. The cyt bc_1 was treated with 10 μM $Q_oC_{10}BrH_2$, 1 mM succinate, and 50 nM SCR to completely reduce [2Fe2S] and cyt c_1 and reduce cyt b_H by 30%. The photo-oxidation and reduction of cyt c_1 was monitored at 552 nm, while the reduction of cyt b_H was monitored at 561−569 nm. Under the conditions used, the reoxidation of cyt b_H by Q in the Q_i site was much slower than reduction because of the low concentration of oxidized Q.

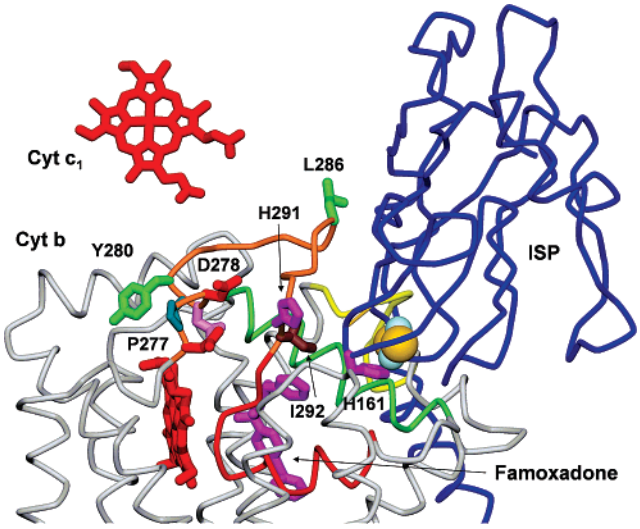

FIGURE 2: X-ray crystal structure of bovine cyt bc_1 with bound famoxadone (*31*). The cyt c_1 and cyt b_L hemes are colored red; the [2Fe2S] center is represented by a CPK model; the ISP is colored blue; and cyt *b* is colored gray. Residues 252−268 in the *ef* loop are colored orange, while residues 269−283 in the PEWY sequence and the *ef* helix are colored red. Residues 136−152 in the cd1 helix are colored green, and residues 163−171 in the neck-contacting domain are colored yellow. The residues in cyt *b* that were mutated are shown as sticks and labeled with *R. sphaeroides* sequence numbering.

RESULTS

The kinetics of electron transfer within *R. sphaeroides* cyt bc_1 were studied using the ruthenium dimer Ru_2D to photoinitiate the reaction (*9*). Laser flash photolysis of a solution containing Ru_2D and cyt bc_1 with cyt c_1 and [2Fe2S] initially reduced resulted in rapid photo-oxidation of cyt c_1, followed by electron transfer from [2Fe2S] to cyt c_1 with a rate constant of $k_1 = 60\,000\ s^{-1}$, monitored at 552 nm (Figure 1) (*9*). The oxidant-induced reduction of cyt b_H monitored at 561−569 nm has a rate constant $k_2 = 2300\ s^{-1}$ (Figure 1), which is rate-limited by electron transfer from QH_2 to [2Fe2S] with rate constant k_2 followed by rapid electron transfer from [2Fe2S] to cyt c_1 and from the semiquinone to cyt b_L and cyt b_H (Scheme 1) (*9*). Binding famoxadone to the Q_o site decreases the rate constant k_1 from 60 000 to 5400 s^{-1}, indicating that the dynamics of rotation of the ISP from the *b* state to the c_1 state was significantly decreased (Figure 1) (*33*). Because famoxadone binding affected the conformation of the *ef* loop in cyt *b*, it was suggested that the *ef* loop might play a role in controlling the conformation of the ISP protein (*31*, *33*). To examine this conformational link further,

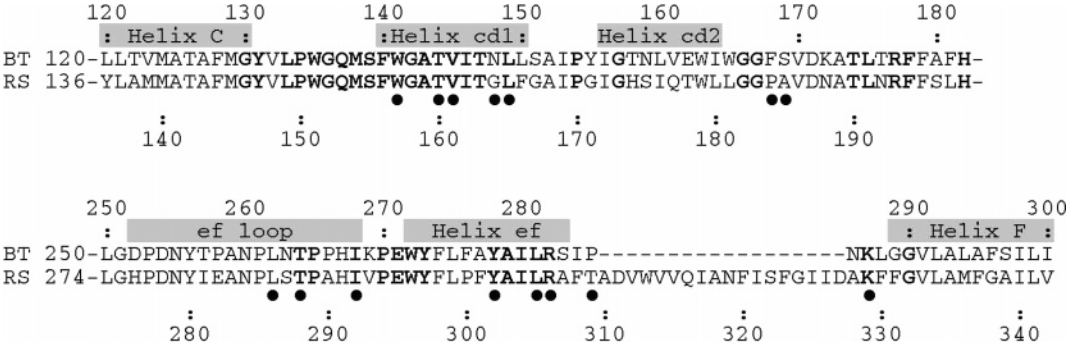

FIGURE 3: Sequence alignment of residues near the Q_o pocket of the cyt *b* subunit in cyt bc_1 complexes from bovine (BT) and *R. sphaeroides* (RS). Residues with a high sequence similarity are in bold font. Helices determined crystallographically are indicated by gray rectangles. Residues in direct contact with the ISP are indicated with a black dot. Adopted from ref *21*.

a series of mutants in which *ef* loop residues were substituted with Ala were prepared. These included the *ef* loop residues H276, P277, D278, N279, Y280, L286, S287, A290, H291, and I292 (Figures 2 and 3). The steady-state activity and the values of the rate constants k_1 and k_2 were measured for each of these mutants, both in the presence and absence of famoxadone. A number of the mutants caused relatively small decreases in the rate constant k_1, but the largest changes were seen for the mutants D278A, Y280A, L286A, and I292A (Table 2). Additional mutants at residues D278, L286, and I292 were prepared to further explore the roles of these residues.

The mutation I292A decreased the steady-state activity from 2.35 to 0.81, k_1 from 60 000 to 4400 s^{-1}, and k_2 from 2300 to 350 s^{-1} (Figure 4A). Famoxadone binding had a relatively small additional effect on k_1, decreasing it only to 3000 s^{-1}. All of the mutations at I292 led to significant decreases in k_1 and k_2 (Table 2). The I292L mutation decreased k_1 to 10 000 s^{-1}, while the I292M mutation decreased k_1 to 6200 s^{-1} (parts B and C of Figure 4). Famoxadone binding had a rather small effect on these two mutants, decreasing k_1 to 4700 and 2800 s^{-1}, respectively. The largest effect was observed for the I292E mutation, which decreased the steady-state activity to 0.12 and eliminated all electron-transfer transients in the ruthenium photo-oxidation experiment. Famoxadone binding eliminated the reduction of cyt b_H observed at 561 nm for all of the mutants, indicating that famoxadone binding was not affected.

The mutation L286A decreased the steady-state rate by 3-fold, k_1 to 33 000 s^{-1}, and k_2 to 740 s^{-1}. Most surprisingly, famoxadone binding did not significantly affect the rate constant k_1, but it did completely inhibit the reduction of cyt b_H. The L286E mutant decreased k_1 to 17 000 s^{-1}, while the addition of famoxadone only decreased k_1 to 12 000 s^{-1}. The conservative mutation L286I decreased k_1 to 18 000 s^{-1}, but famoxadone binding decreased k_1 by a larger factor, to 2900 s^{-1}.

The D278A mutation decreased the steady-state activity from 2.35 to 1.43 and the rate constant k_1 from 60 000 to 26 000 s^{-1} but did not affect the rate constant k_2. Famoxadone binding decreased the rate constant k_1 to 2300 s^{-1}. The mutants D278N, D278E, D278I, and D278H did not have as large of an effect on k_1 or k_2 as the D278A mutation. The Y280A mutation decreased the steady-state activity from 2.35 to 1.34 and the rate constant k_1 from 60 000 to 7900 s^{-1}, without significantly affecting the rate constant k_2. Famoxadone did bind well to this mutant, as indicated by the complete inhibition of the reduction of cyt b_H, but it only decreased the rate constant k_1 from 7900 to 3200 s^{-1}.

Table 2: Effect of the Mutations in the *ef* Loop of cyt *b* on the Kinetics of Electron Transfer within *R. sphaeroides* cyt bc_1

cyt bc_1 mutant[a]	specific activity[b]	famoxadone k_1[c] (s^{-1})	famoxadone k_1 (s^{-1})	k_2[d] (s^{-1})	ΔCA[e] (Å)
wild type	2.35	60 000	5400	2300	
H276A (D252)	1.56	42 000	2800	2200	3.3
P277A (P253)	1.10	35 000	4500	1700	3.0
D278A (D254)	1.43	26 000	2300	2300	2.9
D278N	1.88	35 000	2500	2400	
D278E	1.60	51 000	6700	2900	
D278I	2.41	38 000	4300	2000	
D278H	1.49	36 000	4100	1500	
N279A (N255)	2.43	37 000	4300	1900	1.5
Y280A (Y256)	1.34	7900	3200	2800	0.5
L286A (L262)	0.78	33 000	35 000	740	
L286E	0.88	17 000	12 000	1900	
L286I	2.40	18 000	2900	2300	
S287A (N263)	2.16	55 000	5700	1000	0.7
A290S (P266)	2.65	49 000	5600	1900	0.9
H291A (H267)	2.54	51 000	4100	2000	1.4
I292A (I268)	0.81	4400	3000	350	1.4
I292L	1.30	10 000	4700	1500	
I292M	0.92	6200	2800	1700	
I292V	0.92	33 000	3500	1300	
I292E	0.12				
I292R	0.56	10 000	2 500	1 700	

[a] The corresponding residues of bovine cyt *b* are given in parenthesis. [b] Specific activity is expressed as μmol of cyt *c* reduced min^{-1} (nmol of cyt *b*)$^{-1}$ at 25 °C using chromatophores. The error limits are ±15%. [c] The rate constant k_1 for electron transfer from [2Fe2S] to cyt c_1 was measured at 552 nm in a solution containing 5 μM cyt bc_1, 20 μM Ru_2D, and 5 mM $[Co(NH_3)_5Cl]^{2+}$ in 20 mM sodium borate at pH 9.0 and 0.01% dodecylmaltoside. The cyt bc_1 was treated with 10 μM $Q_oC_{10}BrH_2$, 1 mM succinate, and 50 nM SCR to completely reduce [2Fe2S] and cyt c_1 and reduce cyt b_H by about 30%. Famoxadone (30 μM) was added where indicated. The error limits are ±20%. [d] The rate constant k_2 for electron transfer from QH_2 to [2Fe2S] was measured from the rate of cyt b_H reduction at 561−569 nm under the conditions described for k_1 above. The error limits are ±20%. The addition of famoxadone eliminated the 561−569 nm transients for all of the mutants, indicating that famoxadone bound to all of the mutants in the Q_o pocket. [e] ΔCA is the displacement of the α carbon of the indicated residue in bovine cyt bc_1 induced by famoxadone binding (*31*).

DISCUSSION

Changes in the conformation of the ISP play an essential role in the mechanism of cyt bc_1, and it is important to understand how the dynamics of these conformational changes control electron transfer within the complex. The

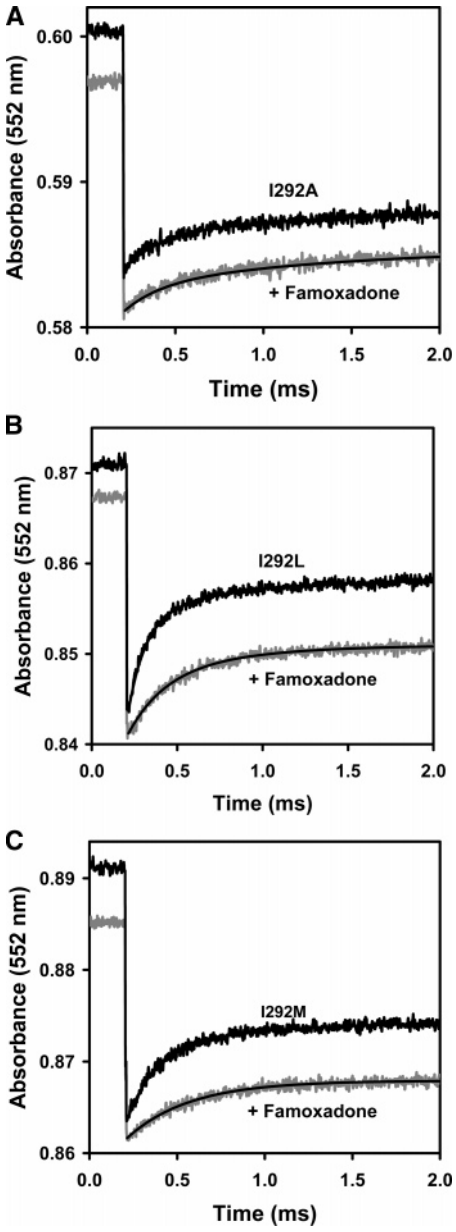

FIGURE 4: Electron transfer from [2Fe2S] to cyt c_1 in *R. sphaeroides* cyt bc_1 mutants following photo-oxidation of cyt c_1. The conditions were the same as described in Figure 1. (A) I292A cyt bc_1. The rate constant k_1 is 4400 s^{-1} in the absence of the inhibitor and 3000 s^{-1} in the presence of 30 μM famoxadone. (B) I292L cyt bc_1. The rate constant k_1 is 10 000 s^{-1} in the absence of the inhibitor and 4700 s^{-1} in the presence of famoxadone. (C) I292M cyt bc_1. The rate constant k_1 is 6200 s^{-1} in the absence of the inhibitor and 2800 s^{-1} in the presence of famoxadone.

ruthenium photo-oxidation technique provides a unique method to measure the rate constants for electron transfer from the [2Fe2S] center to cyt c_1, as well as from QH_2 to the [2Fe2S] center. A number of experiments have indicated that the measured rate constant k_1 for electron transfer from [2Fe2S] to cyt c_1 is rate-limited by a conformational gating mechanism (*33*). If k_1 was rate-limited by true electron transfer from [2Fe2S] to cyt c_1, then the Marcus theory would predict a large dependence on the driving force of the reaction, which depends upon the difference in redox potentials of [2Fe2S] and cyt c_1. However, k_1 is independent of the protonation state of His-161, which significantly affects the redox potential of [2Fe2S] (*33*). Moreover, the rate constant is not affected by ISP mutations, which decrease the redox potential of [2Fe2S] by up to 160 mV (*33*). These studies indicate that the rate constant k_1 provides a direct measure of the dynamics of the conformational change of the ISP from the *b* state and/or the mobile state to the c_1 state (*33*, *42*).

A number of mechanisms have been proposed for the bifurcated electron-transfer reaction at the Q_o site, in which the first electron is transferred from QH_2 to [2Fe2S], while the second electron is transferred from semiquinone to cyt b_L (*21*−*29*). An important requirement for these mechanisms is that they account for the reversibility of the reaction, as well as the minimization of short-circuit reactions, such as the delivery of both electrons from QH_2 to [2Fe2S]. Double-gating mechanisms have been proposed in which QH_2 only reacts at the active Q_o site when the ISP is in the *b* state and both [2Fe2S] and cyt b_L are oxidized (*23*, *25*−*29*). In another proposal, the semiquinone anion moves from the distal site near [2Fe2S] to a position near oxidized cyt b_L to favor electron transfer to the latter (*22*, *27*). Concerted mechanisms have also been proposed in which QH_2 transfers both electrons to [2Fe2S] and cyt b_L simultaneously without the formation of a semiquinone intermediate (*23*, *26*, *28*, *29*). A recent freeze-quench EPR experiment has shown that QH_2 reduces [2Fe2S] and cyt b_L simultaneously with a half-time of 250 μs for a fast phase, which accounts for about 10% reduction of each redox center (*3*). No semiquinone was detected at the Q_o site during oxidation of QH_2, consistent with earlier studies. It is apparent that either the semiquinone intermediate is very short-lived or the bifurcation reaction involves a concerted mechanism.

It has been proposed that a structural linkage between the quinol substrate in the Q_o-binding site and the conformation of the ISP might play an important role in the mechanism of bifurcated electron transfer (*21*). Unfortunately, it has not been possible to experimentally detect QH_2, semiquinone, or Q in the Q_o-binding pocket. Nevertheless, Q_o-site inhibitors have many similarities to the natural ubiquinol substrate, and it has been suggested that the effects of these inhibitors on the conformational linkage between cyt *b* and the ISP might provide insight into the catalytic mechanism of the bifurcation reaction (*21*). X-ray crystallographic studies have shown that Q_o-site inhibitors, including stigmatellin, UHDBT, famoxadone, and JG-144, displace both the cd1 helix and the PEWY sequence in the *ef* helix outward to expand the Q_o pocket and form a binding crater, which captures the ISP in the *b*-state conformation (*21*, *43*). Stigmatellin binding leads to the largest changes in the Q_o pocket and forms a hydrogen bond with the His-161 ligand of the reduced [2Fe2S] center, thus increasing its redox potential by 200−250 mV and completely immobilizing the ISP in the *b* conformation (*5*−*8*, *30*). It has been proposed that QH_2 might bind in a conformation similar to that of stigmatellin, with a hydrogen bond to His-161 to facilitate proton-coupled electron transfer to [2Fe2S] (*22*).

Famoxadone binds somewhat deeper in the Q_o pocket than stigmatellin and does not form a hydrogen bond with His-161 on the ISP (*31*). Even though famoxadone does not contact the ISP, its binding leads to extensive conformational changes on the surface of cyt *b*, which are correlated with the capture of the ISP from the loose state to the *b* state (*31*). These changes include one domain between residues

160−175 (bovine numbering) that contacts the neck region of the ISP, another domain between residues 262 and 268 at the end of the *ef* loop that forms the docking crater for the ISP, and the middle of the *ef* loop (residues 252−256) that connects the Q_o pocket with the other two surface domains (Figures 2 and 3) (*31*). Famoxadone binding to the Q_o site decreases the rate constant k_1 for electron transfer from [2Fe2S] to cyt c_1 from 60 000 to 5400 s^{-1} (*33*). Therefore, famoxadone does not completely lock the ISP in the *b* state but instead significantly decreases the rate of release of the ISP from the *b* state to the c_1 state.

To further explore the role of the *ef* loop in regulating the dynamics of the ISP, a series of mutants at residues in the *ef* loop were constructed. *R. sphaeroides* cyt *b* residues 276−280 correspond to bovine residues 252−256, which are in the middle of the *ef* loop on the surface of cyt *b* (Figures 2 and 3). These residues undergo large displacements upon famoxadone binding, suggesting that they might relay conformational changes in the Q_o pocket to the ISP docking crater. Surprisingly, the mutation of residues H276, P277, D278, and N279 led to relatively small changes in k_1 and k_2, suggesting that, if these residues do help relay conformational changes, then the function is not sensitive to substitution of individual amino acid side changes. The D278A mutation led to the largest decrease in k_1 for this group, from 60 000 to 26 000 s^{-1}, but no significant change in rate constant k_2. Famoxadone binding to this mutant decreased k_1 to 2300 s^{-1}, which is similar to the percent reduction observed in wild-type cyt bc_1, suggesting that this mutant does not modulate the effect of famoxadone. The mutation Y280A led to a substantial decrease in k_1 to 7900 s^{-1}, while famoxadone binding only caused a further decrease to 3200 s^{-1}. This mutation might cause a conformational change similar to that of famoxadone, limiting the additional effect of famoxadone binding.

R. sphaeroides cyt *b* residues 286−292 correspond to bovine residues 262−268 in the *ef* loop, which forms part of the ISP docking crater. The mutation of residues S287, A290, and H291 had relatively little effect on k_1, which is surprising in the case of H291 because the histidine side chain moves 9.3 Å upon famoxadone binding (*31*). However, mutations at I292 located in the ISP docking crater near the [2Fe2S] center had a large effect on electron-transfer activity (Table 2). The I292A mutation decreased k_1 to 4400 s^{-1}, while famoxadone binding only further decreased it to 3000 s^{-1}. The mutations I292L and I292M also led to substantial decreases in k_1, while famoxadone binding caused relatively small additional decreases in k_1. It appears that these mutations significantly decrease the rate of release of the ISP from cyt *b*, but famoxadone binding leads to a relatively small additional decrease in the rate of release. The I292A mutation led to a decrease in the rate constant k_2 for QH_2 oxidation to 350 s^{-1}, indicating that this mutation had an effect on the conformation of the QH_2 reaction site. Substitution of I292 with a basic arginine residue was tolerated with a decrease in k_1 to 10 000 s^{-1} and only a modest change in k_2. In contrast, substitution of I292 with an acidic glutamate nearly completely eliminated both steady-state and electron-transfer activities measured by the ruthenium photo-oxidation method. It is apparent that I292 plays an important role in controlling the conformation of the ISP.

The effects of mutation of L286 at the tip of the *ef* loop are particularly interesting. The mutation L286A decreases the rate constant k_1 to 33 000 s^{-1} and k_2 to 740 s^{-1}. However, famoxadone binding does not lead to any further decrease in k_1 (Table 2), suggesting that this mutation might block the famoxadone-induced conformational change in the wild-type protein, which decreases the rate constant k_1 by such a large factor. The L286E mutation also led to a significant decrease in the rate constant k_1, to 17 000 s^{-1}, while famoxadone binding did not cause much further decrease. The importance of L286 is also illustrated in experiments by Darrouzet and Daldal (*14*, *19*). They found that insertion of one alanine at residue 46 in the neck region of the ISP decreased the rate of the domain movement from the *b* state to the c_1 state to a half-time of 10 ms, which was slow enough to measure in *R. capsulatus* chromatophores. A second revertant mutation substituting Leu for Phe at residue 286 restored rapid domain movement, which was too fast to measure in chromatophores (*19*). This finding is particularly remarkable given that cyt *b* residue 286 is more than 25 Å from the neck region of the ISP. Revertant mutations were also found in the ISP neck region for a primary mutation at T288 in the *ef* loop (*24*). A possible mechanism for this linkage between the *ef* loop and ISP neck region is suggested by the effect of famoxadone binding, which causes correlated conformational changes in both the *ef* loop region and the cyt *b* residues 179−187, which contact the ISP neck region. It appears likely that the conformational linkage between the ISP neck region and the cyt *b ef* loop is mediated by the cyt *b* protein using structural linkages similar to those caused by famoxadone binding.

It has been proposed that the conformation of the ISP plays an important role in several different stages of the mechanism of cyt bc_1 (*21*). First, it is proposed that binding QH_2 to the active Q_o pocket displaces the cd1 and *ef* helixes outward to capture the oxidized ISP in the *b*-state conformation. The formation of a hydrogen bond between QH_2 and His-161 would stabilize the active-site conformation and allow for the proton-coupled electron transfer from QH_2 to oxidize [2Fe2S]. After the second electron is transferred from semiquinone to cyt b_L and cyt b_H, oxidized Q would leave the Q_o-binding pocket and the cd1 and *ef* helixes would relax to their original positions, releasing the ISP and allowing it to rotate to the c_1 position and transfer an electron to cyt c_1 (*21*). An important question about this mechanism is whether ISP is released from the *b* state after the first electron is transferred to [2Fe2S] and the hydrogen bond to His-161 is broken, or whether it remains locked in the *b* state until cyt b_H is reduced. Famoxadone binding is informative in this regard, because it leads to many of the same conformational changes in the ISP-binding crater as stigmatellin but does not form a hydrogen bond to His-161. The rate of release of the ISP from the *b* state is decreased from 60 000 to 5000 s^{-1} by famoxadone binding, but the ISP is not completely locked in the *b* state (*33*). Once the ISP is released from the *b* state and rotates to the cyt c_1 state, there may be conformational linkages that prevent its return to the *b* state under conditions that would lead to short-circuit reactions. When cyt b_H is reduced in the presence of antimycin, an electron is not transferred from cyt *b* to the ISP on a long time scale, suggesting that oxidized ISP does not return to the *b* state in the absence of QH_2. The *ef* loop presents a

barrier to the rotation of the ISP between the *b* and c_1 states (*19*, *32*), and this barrier might regulate the rotation in both directions to facilitate productive electron transfer and prevent short-circuit reactions.

REFERENCES

1. Trumpower, B. L., and Gennis, R. B. (1994) Energy transduction by cytochrome complexes in mitochondrial and bacterial respiration: The enzymology of coupling electron transfer reactions to transmembrane proton translocation, *Annu. Rev. Biochem. 63*, 675−716.
2. Trumpower, B. L. (1990) The protonmotive Q cycle. Energy transduction by coupling of proton translocation to electron transfer by the cytochrome bc_1 complex, *J. Biol. Chem. 265*, 11409−11412.
3. Zhu, J., Egawa, T., Yeh, S.-R., Yu, L., and Yu, C.-A. (2006) Simultaneous reduction of iron−sulfur protein and cytochorme b_L during ubiquinol oxidation in cytochrome bc_1 complex, *Proc. Natl. Acad. Sci. U.S.A.*, in press.
4. Xia, D., Yu, C.-A., Kim, H., Xia, J.-Z., Kachurin, A. M., Zhang, L., Yu, L., and Deisenhofer, J. (1997) Crystal structure of the cytochrome bc_1 complex from bovine heart mitochondria, *Science 277*, 60−66.
5. Zhang, Z., Huang, L., Shulmeister, V. M., Chi, Y.-I., Kim, K. K., Hung, L.-W., Crofts, A. R., Berry, E. A., and Kim, S.-H. (1998) Electron transfer by domain movement in cytochrome bc_1, *Nature 392*, 677−684.
6. Iwata, S., Lee, J. W., Okada, K., Lee, J. K., Wata, M., Rasmussen, B., Link, T. A., Ramaswamy, S., and Jap, B. K. (1998) Complete structure of the 11-subunit bovine mitochondrial cytochrome bc_1 complex, *Science 281*, 64−71.
7. Kim, H., Xia, D., Yu, C.-A., Xia, J.-Z., Kachurin, A. M., Zhang, L., Yu, L., and Deisenhofer, J. (1998) Inhibitor binding changes domain mobility in the iron−sulfur protein of the mitochondrial bc_1 complex from bovine heart, *Proc. Natl. Acad. Sci. U.S.A. 95*, 8026−8033.
8. Hunte, C., Koepke, J., Lange, C., Rossmanith, T., and Michel, H. (2000) Structure at 2.3 Å resolution of the cytochrome bc_1 complex from the yeast *Saccharomyces cerevisiae* co-crystallized with an antibody Fv fragment, *Stucture Fold Des. 8*, 669−684.
9. Sadoski, R. C., Engstrom, G., Tian, H., Zhang, L., Yu, C.-A., Yu, L., Durham, B., and Millett, F. (2000) Use of a photoactivated ruthenium dimer complex to measure electron transfer between the Rieske iron−sulfur protein and cytochrome c_1 in the cytochrome bc_1 complex, *Biochemistry 39*, 4231−4236.
10. Tian, H., Yu, L., Mather, M., and Yu, C. A. (1998) Flexibility of the neck region of the Rieske iron−sulfur protein is functionally important in the cytochrome bc_1 complex, *J. Biol. Chem. 273*, 27953−27959.
11. Xiao, K., Yu, L., and Yu, C.-A. (2000) Confirmation of the involvement of protein domain movement during the catalytic cycle of the cytochrome bc_1 complex by the formation of an intersubunit disulfide bond between cytochrome *b* and the iron−sulfur protein, *J. Biol. Chem. 275*, 38597−38604.
12. Tian, H., White, S., Yu, L., and Yu, C.-A. (1999) Evidence for the head domain movement of the Rieske iron−sulfur protein in electron transfer reaction of the cytochrome bc_1 complex, *J. Biol. Chem. 274*, 7146−7152.
13. Darrouzet, E., Valkova-Valchanova, M., and Daldal, F. (2000) Probing the role of the Fe−S subunit hinge region during Q_o site catalysis in *Rhodobacter capsulatus* bc_1 complex, *Biochemistry 39*, 15475−15483.
14. Darrouzet, E., Valkova-Valchanova, M., Moser, C. C., Dutton, P. L., and Daldal, F. (2000) Uncovering the [2Fe2S] domain movement in cytochrome bc_1 and its implications for energy conversion, *Proc. Natl. Acad. Sci. U.S.A. 25*, 4567−4572.
15. Nett, J. H., Hunte, C., and Trumpower, B. L. (2000) Changes to the length of the flexible linker region of the Rieske protein impair the interaction of QH_2 with the cytochrome bc_1 complex, *Eur. J. Biochem. 267*, 5777−5782.
16. Gosh, M., Wang, C., Ebert, E., Vadlamuri, S., and Beattie, D. S. (2001) Substituting leucine for alanine-86 in the tether region of the iron−sulfur protein of the cytochrome bc_1 complex affects the mobility of the [2Fe2S] domain, *Biochemistry 40*, 327−335.
17. Engstrom, G., Xiao, K., Yu, C.-A., Yu, L., Durham, B., and Millett, F. (2002) Photoinduced electron transfer between the Rieske iron−sulfur protein and cytochrome c_1 in the *Rhodobacter sphaeroides* cytochrome bc_1 complex. Effects of pH, temperature, and driving force, *J. Biol. Chem. 277*, 31072−31078.
18. Darrouzet, E., Valkova-Valchanova, M., and Daldal, F. (2002) The [2Fe−2S] cluster E_m as an indicator of the iron−sulfur subunit position in the ubihydroquinone oxidation site of the cytochrome bc_1 complex, *J. Biol. Chem. 277*, 3464−3470.
19. Darrouzet, E., and Daldal, F. (2002) Movement of the iron−sulfur subunit beyond the *ef* loop of cytochrome *b* is required for multiple turnovers of the bc_1 complex but not for a single turnover Q_o site catalysis, *J. Biol. Chem. 277*, 3471−3476.
20. Brugna, M., Rodgers, S., Schricker, A., Montoya, G., Kazmeier, M., Nitschike, W., and Sinning, I. (2000) A spectroscopic method for observing the domain movement of the Rieske iron−sulfur protein, *Proc. Natl. Acad. Sci. U.S.A. 97*, 2069−2074.
21. Esser, L., Gong, X., Yang, S., Yu, L., Yu, C.-A., and Xia, D. (2006) Surface-modulated motion switch: Capture and release of iron−sulfur protein in the cytochrome bc_1 complex, *Proc. Natl. Acad. Sci. U.S.A. 103*, 13045−13050.
22. Hong, S., Ugulava, N., Guergova-Kuras, M., and Crofts, A. R. (1999) The energy landscape for ubihydroquinone oxidation at the Q_o site of the bc_1 complex in *R. sphaeroides*, *J. Biol. Chem. 274*, 33931−33944.
23. Osyczka, A., Moser, C. C., Daldal, F., and Dutton, P. L. (2004) Reversible redox energy coupling in electron transfer chains, *Nature 427*, 607−612.
24. Darrouzet, E., and Daldal, F. (2003) Protein−protein interactions between cytochrome *b* and the Fe−S protein subunits during QH_2 oxidation and large-scale domain movement in the bc_1 complex, *Biochemistry 42*, 1499−1507.
25. Rich, P. (2004) The quinine chemistry of *bc* complexes, *Biochim. Biophys. Acta 1658*, 165−171.
26. Osyczka, A., Moser, C. C., and Dutton, P. L. (2005) Fixing the Q cycle, *Trends Biochem. Sci. 30*, 176−182.
27. Crofts, A. R., Lhee, S., Crofts, S. B., Cheng, J., and Rose, S. (2006) Proton pumping in the bc_1 complex: A new gating mechanism that prevents short circuits, *Biochim. Biophys. Acta*, Epub ahead of print.
28. Mulkidjanian, A. Y. (2005) QH_2 oxidation in the cytochrome bc_1 complex: Reaction mechanism and prevention of short-circuiting, *Biochim. Biophys. Acta 1709*, 5−34.
29. Osyczka, A., Zhang, H., Mathe, C., Rich, P. R., Moser, C. C., and Dutton, P. L. (2006) Role of the PEWY glutamate in hydroquinone−quinone oxidation−reduction catalysis in the Q_o site of cytochrome bc_1, *Biochemistry 45*, 10492−10503.
30. von Jagow, G., and Ohnishi, T. (1985) The chromone inhibitor stigmatellin-binding to the QH_2 oxidation center at the C-side of the mitochondrial membrane, *FEBS Lett. 185*, 311−315.
31. Gao, X. Wen, X., Yu, C.-A., Esser, L., Tsao, S., Quinn B., Zhang, L., Yu, L., and Xia, D. (2002) The crystal structure of mitochondrial cytochrome bc_1 in complex with famoxadone: The role of aromatic−aromatic interaction in inhibition, *Biochemistry 41*, 11692−11702.
32. Izrailev, S., Crofts, A. R., Berry, E. A., and Schulten, K. (1999) Steered molecular dynamics simulation of the Rieske subunit motion in the cytochrome bc_1 complex, *Biophys. J. 77*, 1753−1768.
33. Xiao, K., Engstrom, G., Rajagukguk, S., Yu, C.-A., Yu, L., Durham, B., and Millett, F. (2003) Effect of famoxadone on photoinduced electron transfer between the iron−sulfur center and cytochrome c_1 in the cytochrome bc_1 complex, *J. Biol. Chem. 278*, 11419−11426.
34. Downard, A. J., Honey, G. E., Phillips, L. F., and Steel, P. J. (1991) Synthesis and properties of a tris(2,2′-bipyridine)ruthenium(II) dimer directly coupled at the C4 carbon, *Inorg. Chem. 30*, 2259−2260.
35. Moeller, T., Ed. (1957) *Inorganic Synthesis*, Vol. 5, p 185, McGraw Hill Book Company, Inc., New York.
36. Yu, C. A., and Yu, L. (1982) Syntheses of biologically active ubiquinone derivatives, *Biochemistry 21*, 4096−4101.
37. Yu, L., and Yu, C. A. (1982) Quantitative resolution of succinate−cytochrome *c* reductase into succinate−ubiquinone and QH_2−cytochrome *c* reductases, *J. Biol. Chem. 257*, 2016−2021.
38. Mather, M. W., Yu, L., and Yu, C.-A. (1995) The involvement of threonine 160 of cytochrome *b* of *Rhodobacter sphaeroides* cytochrome bc_1 complex in quinone binding and interaction with subunit IV, *J. Biol. Chem. 270*, 28668−28675.

39. Xiao, K., Yu, L., and Yu, C.-A. (2000) Confirmation of the involvement of protein domain movement during the catalytic cycle of the cytochrome bc_1 complex by the formation of an intersubunit disulfide bond between cytochrome *b* and the iron−sulfur protein, *J. Biol. Chem. 275*, 38597−38604.
40. Liu, X., Yu, C. A., and Yu, L. (2004) The role of extra fragment at the C-terminal of cytochrome *b* (residues 421−445) in the cytochrome bc_1 complex from *Rhodobacter sphaeroides*, *J. Biol. Chem. 279*, 47363−47371.
41. Heacock, C., Liu, R., Yu, C.-A., Yu, L., Durham, B., and Millett, F. (1993) Intracomplex electron transfer between ruthenium−cytochrome *c* derivatives and cytochrome c_1, *J. Biol. Chem. 268*, 27171−27175.
42. Yu, C. A., Wen, X., Xiao, K., Xia, D., and Yu, L. (2002) Inter- and intra-molecular electron transfer in the cytochrome bc_1 complex, *Biochim. Biophys. Acta 1555*, 65−70.
43. Esser, L., Quinn, B., Li, Y. F., Zhang, M., Elberry, M., Yu, L. Yu, C. A., and Xia, D. (2004) Crystallographic studies of quinol oxidation site inhibitors: A modified classification of inhibitors for the cytochrome bc_1 complex, *J. Mol. Biol. 341*, 281−302.

BI062094G